

**Waveguide evanescent field fluorescence  
microscopy: high contrast imaging of a  
domain forming mixed lipid  
Langmuir-Blodgett monolayer mimicking  
lung surfactant**

Abdollah Hassanzadeh  
Silvia Mittler

# Waveguide evanescent field fluorescence microscopy: high contrast imaging of a domain forming mixed lipid Langmuir-Blodgett monolayer mimicking lung surfactant

Abdollah Hassanzadeh\* and Silvia Mittler

University of Western Ontario, Department of Physics and Astronomy, London, Ontario, N6A 3K7 Canada

**Abstract.** Waveguide evanescent field fluorescence (WEFF) microscopy is a new development that allows the imaging of contact regions between biological cells and their substratum, as well as imaging of ultrathin films such as monomolecular Langmuir-Blodgett (LB) films. Mixed-lipid monolayer systems mimicking lung surfactant were fabricated on waveguides using the LB technique and imaged by both WEFF and standard wide field epifluorescence microscopy. These two technologies were compared with respect to contrast, photobleaching, and sensitivity. It was found that WEFF microscopy produced images with a much higher contrast, lower photobleaching, and higher sensitivity. In addition, fine structures in the lipidic domains were observed for the first time. © 2011 Society of Photo-Optical Instrumentation Engineers (SPIE). [DOI: 10.1117/1.3569095]

Keywords: fluorescence microscopy; evanescent microscopy; Langmuir-Blodgett films; lipids; sensitivity; photobleaching; contrast.

Paper 10608LR received Nov. 16, 2010; revised manuscript received Feb. 25, 2011; accepted for publication Feb. 28, 2011; published online Apr. 29, 2011; corrected May 6, 2011.

## 1 Introduction

Waveguide evanescent field fluorescence (WEFF) microscopy<sup>1-8</sup> selectively excites fluorophores very near to a glass surface (<100 nm). The intensity of this thin zone of electromagnetic wave decays exponentially from the glass surface and its intensity maximum is located at the waveguide-cover medium interface. In this particular case, the penetration depth of the evanescent field is ~60 nm for the TE<sub>0</sub> mode in the waveguide used. This results in images with very low background fluorescence, a very high axial resolution, and minimal exposure of the sample to light at any other plane. Since the deposited lipid Langmuir-Blodgett (LB) monolayer's thickness is much smaller than the penetration depth of the evanescent field, all of the fluorophores in the monolayer become excited, and this allows for the construction of images of high contrast dye distribution.

WEFF microscopy can be used to image the focal adhesions of living cells and to measure the distance of the focal adhesion to the waveguide surface.<sup>4,5</sup> WEFF microscopy and total internal reflection fluorescence microscopy<sup>8,9</sup> both deliver the same images of cells and exhibit similar scattering background contributions. In this letter, we would like to show how WEFF microscopy can contribute to ultrathin film research. These contributions include quality control investigations and dynamic studies, such as film homogeneity and monolayer formation, as well as providing answers to engineering questions relating to durability and long-term stability or aging.

In WEFF microscopy, a commercial inverted microscope is used. A laser ( $\lambda = 543.5$  nm, 0.5 mW) is coupled into a

waveguide mode with a photoresist coupling grating. The waveguide is mounted on the sample stage of the microscope and a 560-nm long pass filter is applied to block the excitation wavelength. Images are obtained by employing a software-operated digital camera. The waveguides containing the coupling gratings are not yet commercially available but are individually fabricated and characterized by using ion exchange and photoresist technologies. The only two critical parameters in waveguide design are to first decide the wavelength of operation, which depends on the dye used for the specimen under study, and then to achieve the appropriate coupling angle spectrum for the grating. It is important to direct the laser beam unobstructed onto the coupling grating between 34 deg and 70 deg from underneath the microscope's sample stage.

A monolayer consisting of lipids and proteins, called "lung surfactant," covers the air-water interface at the alveoli in the lungs and provides low surface tension necessary for normal pulmonary function and for minimizing the work requirement for breathing.<sup>10,11</sup> Lung surfactant is a complex mixture of lipids and proteins that is difficult to mimic in an artificial setting. Various mixtures of dipalmitoyl-phosphatidylcholine (DPPC), unsaturated phosphatidylglycerols (PG), palmitic acid (PA), and 1-palmitoyl-2-oleyl-phosphatidylglycerols (POPG) were prepared to simulate the main lipid components found in lung surfactant.<sup>12-14</sup>

We have chosen this artificial lung surfactant system as a model system to study the advanced imaging possibilities of WEFF microscopy. It is known from fluorescence microscopy that this lipid mixture exhibits condensed, DPPC/PA-enriched domains in a continuous, liquid-expanded DPPC-POPG matrix, which leads to distinct morphologies at low surface pressures.<sup>14</sup> LB monolayers at the air-water interface were used as an acceptable and accessible model for studies of lung surfactants. The lipid composition of this lung surfactant model was

\*Current affiliation: University of Kurdistan, Department of Physics, Sanandaj, Kurdistan, Iran.

Address all correspondence to: Silvia Mittler, University of Western Ontario, Physics and Astronomy, Middlesex Drive, London, Ontario, N6A 3K7 Canada. Tel: 519 661 2111; Fax: 519 661 2033; E-mail: smittler@uwo.ca.

imaged by fluorescence and Brewster angle microscopy.<sup>15–17</sup> Since the thickness of the Langmuir–Blodgett film is  $\sim 2.5$  nm, the implementation of an evanescent microscopy technology should reveal more information about the lipid domain morphology than “transmission-based” fluorescence microscopy.

Monolayers of the model lung surfactant system as described by Bringezu et al.<sup>12,13</sup> were deposited onto glass waveguides by means of the LB method at various surface pressures,  $\Pi$ . A custom-built WEFF microscope<sup>4</sup> was used to image the DiI-stained monolayers. Parallel to WEFF microscopy, images of the same samples were also obtained using a standard wide field epi-fluorescence microscope (Zeiss Axio Imager Z1 Microscope, Germany). In comparison to standard microscopy, WEFF microscopy produced images with higher contrast and sensitivity, and with lower photobleaching. A more detailed analysis of the morphology of a given monolayer film was made possible due to the increase in contrast and axial resolution.

## 2 Results and Discussion

### 2.1 Surface Pressure–Area Isotherm

Figure 1 shows the surface pressure–area isotherm of the lipid mixture at the air–water interface at room temperature. The surface pressure,  $\Pi$ , began to increase at  $\sim 58$  Å<sup>2</sup>/molecule and increased up to 40 mN/m. This was followed by a plateau between 40 and 44 mN/m. Upon further compression, the lipids showed a steep pressure increase before finally collapsing at 57 mN/m. These findings were similar to the results presented in the study conducted by Bringezu et al.<sup>12,13</sup> on the influence of the concentration of added PA, but in addition showed a plateau which is not shown by Bringezu for that particular lipid mixture.

### 2.2 WEFF and Conventional Wide Field Epi-Fluorescence Microscopy

The morphology of a mixed-lipid monolayer film can be altered by changing the surface pressure of this film on the LB trough.<sup>16,17</sup> Before the development of WEFF microscopy, a typ-

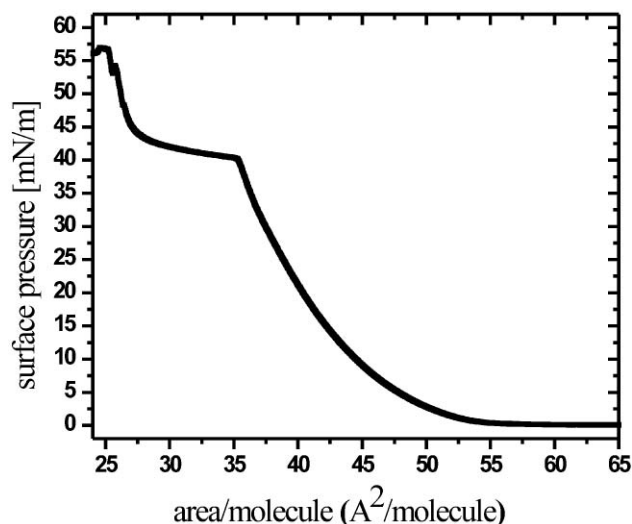


**Fig. 1** Surface pressure–area isotherm for the lipid mixture of DPPC/POPG/PA with a ratio of (62/18/20 vol/vol/vol) at 23°C on a subphase of pure water.

ical domain image was obtained using fluorescence or Brewster angle microscopy as a dark matrix with bright spots or vice versa, depending on the pressure and composition of the monolayer.<sup>17</sup> In this study, WEFF and wide field epi-fluorescence microscopy were used to investigate the morphologies of mixed-lipid LB films on waveguides at different surface pressures (5, 10, 20 and 43 mN/m). Figure 2 shows the WEFF (left column) and epi-fluorescence (right column) microscopy images at identical magnification of LB films at various surface pressures. Both WEFF and standard fluorescence microscopy images of transferred mixed lipid films at 5 mN/m showed bright and circular “liquid” phase regions in a continuous, condensed phase. This bright “liquid” phase covered around 80% of the total area of the film. At  $\Pi = 10$  mN/m, the bright, liquid phase circles disappeared and dark, condensed domains appeared in a continuous and bright “liquid” phase. This is a transition appearing at surface pressures higher than 8 mN/m.<sup>12,13</sup> These dark domains covered around 30% of the total area of the film. By increasing  $\Pi$  to 20 mN/m, the bright “liquid” phase penetrated into the dark condensed domains. The number of dark condensed domains decreased and their average size increased. They covered 25%

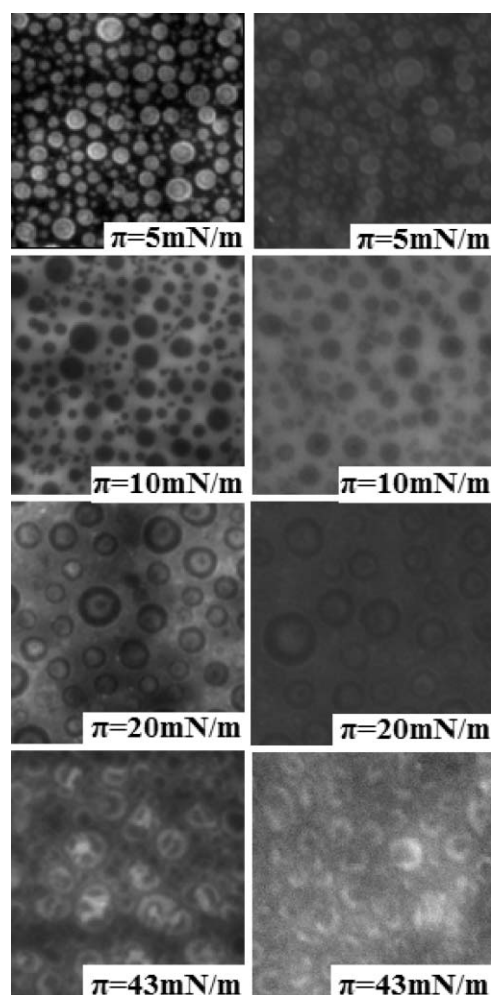


**Fig. 2** WEFF (left column) and epi-fluorescence microscopy (right column) images of transferred lipid mixture DPPC/POPG/PA (62/20/18; vol/vol/vol) to a waveguide surface using the LB technique. The images were taken at 23°C. The width of each image is 50  $\mu$ m.

of the total area of the film. At 43 mN/m, the WEFF microscopy image showed dark domains having lost their circularity and having developed internal, bright “liquid” phase structures.

### 2.3 Lipid Mixture on Water and Transferred onto a Solid Substrate

The fluorescence microscopy images of the lipid mixture produced by Bringezu et al.<sup>12,13</sup> at the air–water interface at 5 mN/m showed a bright liquid phase in a continuous dark phase. For pressures >8 mN/m, they found the above-mentioned transition between liquid and condensed phases. For surface pressures of 5 and 10 mN/m, our results with both WEFF and fluorescence microscopy were in perfect agreement with those of Bringezu et al.<sup>12,13</sup> The same transition was detected for surface pressures >8 mN/m. At the higher surface pressures of 20 and 43 mN/m, both WEFF and epi-fluorescence microscopes images showed a bright “liquid” phase penetrating into the dark domains. The shape of the bright liquid phase inside the dark domains depends on the size of the dark domains and on the surface pressure. For example, at 20 mN/m, the small-size domains have bright, circular shapes covering the middle part of the domains, whereas the large-size domains have a ring structure at their centers. At surface pressure of 43 mN/m, the internal structures of the domains are more complex and are closer together. WEFF microscopy images showed that the concentration of the “liquid” phase inside the dark domains is higher than that outside. It is assumed as a first approximation that the film morphology and inner structure does not change with the LB transfer. However, the liquid phase on the air–water interface after LB transfer is not necessarily a “liquid” on the substrate. Therefore, the word “liquid” is presented in quotation marks.

### 2.4 WEFF and Conventional Wide Field Epi-Fluorescence Microscopy

In comparing the two columns of images of the transferred LB films (Fig. 3), WEFF microscopy was found to produce images

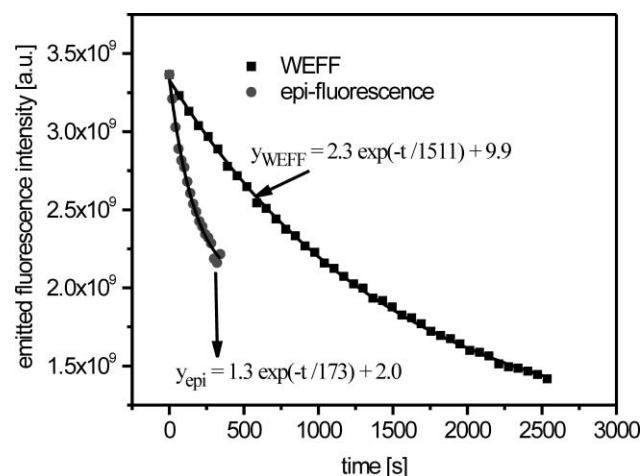


**Fig. 3** Measured integrated emitted fluorescence intensity over time for WEFF (□) microscopy and epi-fluorescence microscopy (●). The lines are fitted exponential decay functions. The fluorescence intensity decreases with a decay constant of 1511 s for WEFF microscopy and 173 s for epi-fluorescence.

with enhanced contrast and higher overall brightness. For example, the circular regions showed sharper edges at all surface pressures studied. At  $\Pi = 5$  and 43 mN/m, the WEFF microscopy images demonstrated for the first time that the circular liquid phase regions have an internal fine structure. In contrast, some of the condensed domains in the images produced by epi-fluorescence microscopy could not be recognized at 20 mN/m. At 43 mN/m, the domains lacked clear edges and the internal structures were no longer identifiable. In the past, images of this lung surfactant model system taken at the air–water interface using Brewster angle and fluorescence microscopies did not reveal any internal structure in the domains.<sup>12,13</sup> The question still remains whether this internal structure is present at the air–water interface but was not able to be observed, or whether it is an artifact resulting from the transfer of the lipid mixture onto the solid substrate. However, this problem cannot be answered at this point and is also not the focus of this microscopy-related study.

### 2.5 Photobleaching

Photo bleaching is of major concern in any fluorescence microscopy technology. It reduces observation time. This problem becomes especially critical for any quantitative application of fluorescence microscopy and in kinetic studies. In WEFF microscopy, only a thin film of the stained specimen is illuminated by the evanescent field. This should reduce the photobleaching in comparison to epi-fluorescence microscopy. In order to compare the rate of photobleaching, a series of images was captured for both microscopy methods under their individual optimal illumination and imaging conditions. The integrated intensities along the area of the entire image were measured (Image J). Figure 3 shows the integrated intensities of both microscopy technologies with respect to the exposure time. In both cases, the fluorescence intensity decayed with increasing exposure time. However, WEFF microscopy clearly exhibited a weaker decay. The intensity curves were fitted to an exponential decay function (see Fig. 3 for details). Under the applied conditions, epi-fluorescence microscopy was able to be conducted for 5 min, whereas WEFF microscopy allowed an imaging time of 43 min. The lowest data points in both data sets represent the integrated intensities of images in which the image features cannot be clearly observed as a result of the contrast disappearing almost completely. For standard epi-fluorescence microscopy, this intensity is two times greater in comparison to WEFF microscopy. This is an excellent indication of a softer illumination in WEFF microscopy as compared to epi-fluorescence microscopy. It also confirms the higher sensitivity and contrast exhibited in images produced by WEFF microscopy.

## 3 Conclusion

In conclusion, the LB technique was used to deposit a stained, phase-separated monolayer, which serves as a model system for lung surfactant, onto waveguides at four different surface pressures. Images of these films at various surface pressures were captured using both WEFF and wide-field epi-fluorescence microscopy. It was found that WEFF microscopy offered higher contrast, better sensitivity, and lower photobleaching. An internal fine structure in both bright “liquid” ( $\Pi = 5$  mN/m) and condensed phases were observed for the first time in WEFF mi-

croscopy images. WEFF microscopy can be a helpful tool in the future for addressing fundamental scientific and engineering questions in thin film research.

### Acknowledgments

We would like to acknowledge the Western Nanofabrication Laboratory for hosting our LB-trough and our laser holography, and for the availability of the photoresist technology. Minh Luan (David) Quach is thanked for critically reading the manuscript. S.M. would like to thank the CRC program of the Canadian Government. The authors would like to thank NSERC, CFI, and OIF for financial support. The Biotron Imaging Suite at Western, especially Richard Harris, is thanked for their help with the Zeiss Axio Imager Z1 Microscope.

### References

1. S. Mittler, "Imaging of Thin Films and its Application in Life Sciences," in *Nanostructures Thin Films for Life Sciences*, C. Kumar, Ed., Wiley-VCH Series "Nanomaterials for the Life Sciences" Vol. 5, pp. 363–395 (2010).
2. H. M. Grandin, B. Städtler, M. Textor, and J. Vörös, "Waveguide excitation fluorescence microscopy: a new tool for sensing and imaging the biointerface," *Biosens. Bioelectron.* **21**(8), 1476–1482 (2006).
3. R. Horvath, H. C. Pedersen, N. D. Selmeczi, and N. B. Larsen Skivesen, "Monitoring of living cell attachment and spreading using reverse symmetry waveguide sensing," *Appl. Phys. Lett.* **86**, 071101 (2005).
4. A. Hassanzadeh, M. Nitsche, S. Armstrong, J. Dixon, U. Langbein, and S. Mittler, "Waveguide evanescent field fluorescence microscopy: Thin film fluorescence intensities and its application in cell biology," *Appl. Phys. Lett.* **92**(23), 233503 (2008).
5. A. Hassanzadeh, S. Armstrong, S. J. Dixon, and S. Mittler, "Multimode waveguide evanescent field fluorescence microscopy: Measurement of cell-substratum separation distance," *Appl. Phys. Lett.* **94**(3), 033503 (2009).
6. B. Agnarsson, S. Ingthorsson, T. Gudjonsson, and K. Leosson, "Evanescent-wave fluorescence microscopy using symmetric planar waveguides," *Opt. Express* **17**(7), 5075–5082 (2009).
7. A. Hassanzadeh, H. K. Ma, S. Armstrong, S. J. Dixon, S. M. Sims, and S. Mittler, "Waveguide evanescent field fluorescence microscopy: from cell-substratum distances to kinetic cell behaviour," *Proc. SPIE* **7322**, 73220 (2009).
8. A. Hassanzadeh, M. Nitsche, S. Armstrong, N. Nabavi, R. Harrison, S. J. Dixon, U. Langbein, and S. Mittler "Optical waveguides formed by silver ion exchange in Schott SG11 glass for waveguide evanescent field fluorescence microscopy: evanescent images of HEK293 cells," *Biomed. Opt.* **15**(3), 036018 (2010).
9. D. Axelrod, "Total internal reflection fluorescence microscopy," in *Biophysical Tools for Biologists, Vol. 2, In Vivo Techniques, Methods Cell Biol.* **89**, 169–221 (2008).
10. S. Schurch, J. Goerke, and J. A. Clements, "Direct determination of surface-tension in lung" *Proc. Natl. Acad. Sci. U.S.A.* **73**(12), 4698–4702 (1976).
11. J. Goerke, "Pulmonary surfactant: functions and molecular composition" *Biochem. Biophys. Acta* **1408**(2–3), 79–89 (1998).
12. F. Bringezu, J. Ding, G. Brezesinski, and J. A. Zasadinski, "Changes in model lung surfactant monolayers induced by palmitic acid," *Langmuir* **17**(15), 4641–4648 (2001).
13. F. Bringezu, K. E. Pinkerton, and J. A. Zasadinski, "Environmental tobacco smoke effects on the primary lipids of lung surfactant," *Langmuir* **19**(7), 2900–2907 (2003).
14. H. Nakahara, S. Lee, G. Sagihara, C.-H. Chang, and O. Shibata, "Langmuir monolayer of artificial pulmonary surfactant mixtures with an amphiphilic peptide at the air/water interface: Comparison of new preparations with surfacten (Surfactant TA)," *Langmuir* **24**(7), 3370–3379 (2008).
15. R. Veldhuizen, K. Nag, S. Orgeug, and F. Possmayer, "The role of lipids in pulmonary surfactant," *Biochem. Biophys. Acta* **1408**(2–3), 90–108 (1998).
16. H. McConnell, "Structures and transitions in lipid mololayers at the air-water-interface," *Annu. Rev. Phys. Chem.* **42**, 171–195 (1991).
17. M. M. Lipp, K. Y. C. Lee, J. A. Zasadinski, and A. Waring, "Design and performance of an integrated fluorescence, polarized fluorescence, and Brewster angle microscope Langmuir trough assembly for the study of lung surfactant monolayers," *J. Rev. Sci. Instrum.* **68**(6), 2574–2582 (1997).